CONF-800723--3

LA-UR -80-716, FINAL

TITLE: TRAC POSTTEST CALCULATIONS OF SEMISCALE TEST S-06-3

MASTER

AUTHOR(S): John R. Ireland, Q-6
Paul B. Bleiweis, Science Applications, Inc.

SUBMITTED TO: ASME 1980 NATIONAL HEAT TRANSFER CONFERENCE
Orlando, Florida
July 27-30, 1980

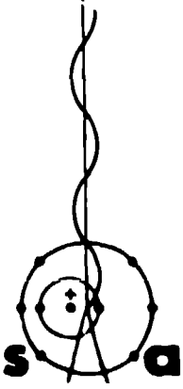

los alamos
scientific laboratory
of the University of California
LOS ALAMOS, NEW MEXICO 87545

An Affirmative Action/Equal Opportunity Employer

Form No. 836 R2
St. No. 2629
1/78

DEPARTMENT OF ENERGY
CONTRACT W-7405-ENG. 36

TRAC POSTTEST CALCULATIONS OF SEMISCALE TEST S-06-3[1]

by

John R. Ireland and Paul B. Bleiweis[2]
Energy Division
Los Alamos Scientific Laboratory
University of California
Los Alamos, New Mexico 87545

ABSTRACT

A comparison of Transient Reactor Analysis Code (TRAC) steady-state and transient results with Semiscale Test S-06-03 (U.S. Standard Problem 8) experimental data is discussed. The TRAC model used employs fewer mesh cells than normal data comparison models so that TRAC's ability to obtain reasonable results with less computer time can be assessed. In general, the TRAC results are in good agreement with the data and the major phenomena found in the experiment are reproduced by the code with a substantial reduction in computing times.

INTRODUCTION

TRAC (1) is a computer code, developed by the Los Alamos Scientific Laboratory, which is capable of simulating transients in both experiments and full-scale pressurized water reactors (PWRs). Initial code versions were designed to calculate large-break (200%, double-ended ruptures) loss-of-coolant accidents (LOCAs) in various systems. Because the code employs a three-dimensional geometric representation in the pressure vessel and a one-dimensional simulation of the balance of the primary system, most TRAC system calculations contain a large number of fluid mesh cells (e.g., 700 to 800 cells for a typical fine-node PWR calculation). Running times for such calculations can be quite long, particularly if there are many three-dimensional cells. To assess TRAC's ability to produce reasonable results with a reduction in mesh cells (and running time), steady-state and transient TRAC calculations of Semiscale Test S-06-3 (U.S. Standard Problem 8) were performed with a model containing fewer TRAC cells than are normally used for calculations of this type.

Test S-06-3 is a particularly good test to model for this study because it was a full 200% break LOCA running from blowdown through reflood. Thus, all of the important phenomena encountered during a typical PWR LOCA are present in this Semiscale test.

TRAC MODEL OF THE SEMISCALE SYSTEM

Figure 1 shows a TRAC schematic of the Semiscale system, which was modeled by 15 TRAC components and 15 junctions. The vessel noding is shown in Fig. 2 and the axial power distribution is shown in Fig. 3. Three axial core levels were used to model the axial power shape. Because two azimuthal segments and one radial ring were used in the core region, two average power rods along with a high-power and a low-power rod were used for heat transfer and peak clad temperature calculations. A total of 112 TRAC cells (24 cells in the vessel) were used to model the system. As mentioned above, the noding was reduced from that normally employed for detailed calculations. The emergency core cooling (ECC) system flows were modeled with a fill component by combining the measured accumulator, low-pressure injection system (LPIS), and high-pressure injection system (HPIS) volumetric flows to obtain an effective ECC velocity vs time. This curve is shown in Fig. 4. The break nozzle noding for both the broken cold leg and broken hot leg is shown in Fig. 5, and the simulated containment suppression tank back pressure, modeled as a break component in TRAC, is shown in Fig. 6. This pressure boundary condition was used on both the broken hot leg and the broken cold leg.

There are a few potential problems associated with the reduction in noding of the system described above. The use of only three axial core levels may lead to problems during the reflood stage of the transient because the fluid mesh cells are large and the axial power shape, shown in Fig. 3, is much coarser than in the actual experiment. Two azimuthal segments, instead of the usual four, may smear some of the flows to an extent that deviations between the experimental data and the TRAC results may occur.

RESULTS

The steady-state option in TRAC was used to generate initial conditions before transient initiation. These calculated conditions are compared with the measured data (2) in Table I. As can be seen, the agreement between the measured and the TRAC calculated conditions is good. Table II summarizes some of the important events that occurred during the transient calculation. The calculation was stopped at 250 s after the high-power rod quenched through the core midplane. These events calculated by TRAC are generally in good agreement with the experimental results.

A comparison of the calculated and the experimental upper plenum pressure is shown in Fig. 7 for the first 40 s of the transient. This comparison shows that TRAC slightly underpredicts the pressure for most of the blowdown, however, the agreement is still quite good. The difference can be attributed to the coarse noding in the core and the two-pin approximation that was made to obtain the axial power shape. These effects cause the power in the central high-power region to be lower than in the actual case, resulting in a lower vessel pressure.

Comparisons of the intact loop pump inlet density and cold leg density are shown in Figs. 8 and 9. Both comparisons show good agreement between the calculated and the experimental values over most of the transient. However, as can be seen from Fig. 9, the

[1]Work performed under the auspices of the U.S. Nuclear Regulatory Commission.

[2]Present address: Science Applications, Inc., 200 Louisa, N.W., Suite 600, Albuquerque, New Mexico 87102.

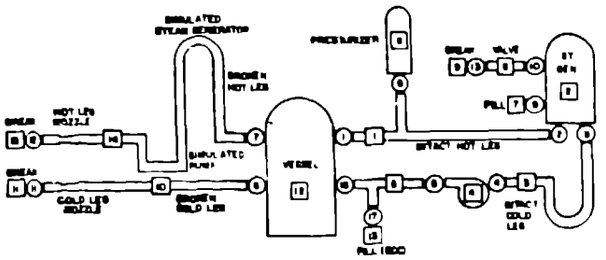

Fig. 1. TRAC schematic of Semiscale system.

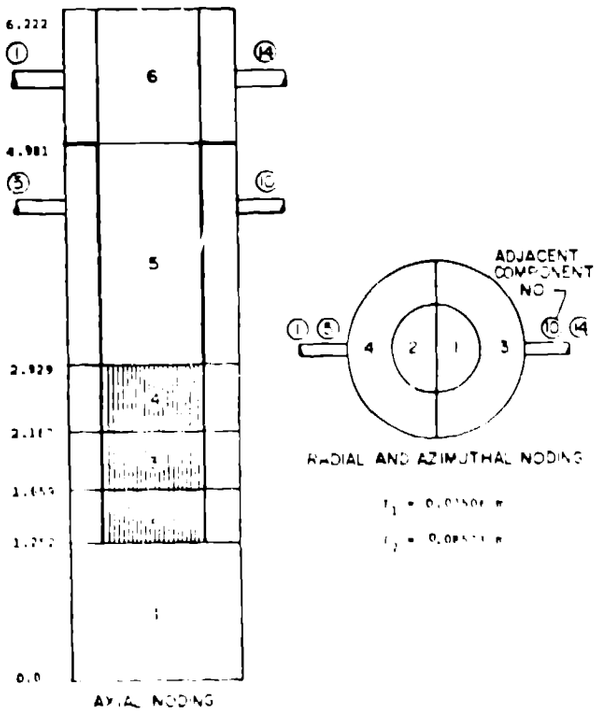

Fig. 2. TRAC vessel noding.

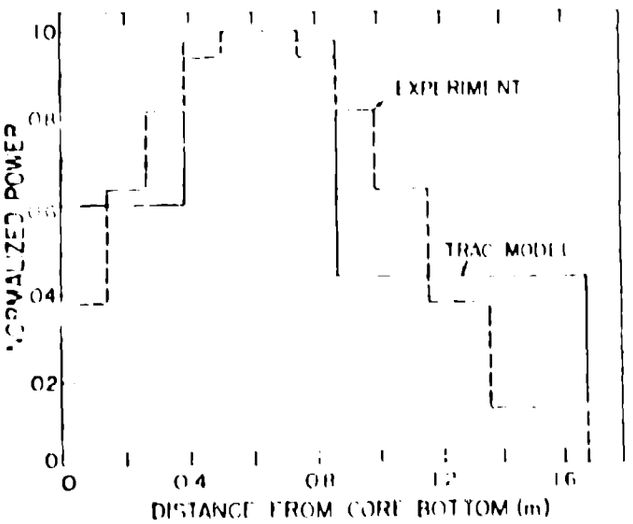

Fig. 3. Axial power distribution.

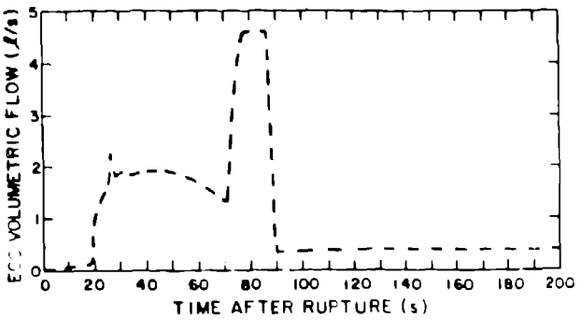

Fig. 4. ECC flow rate.

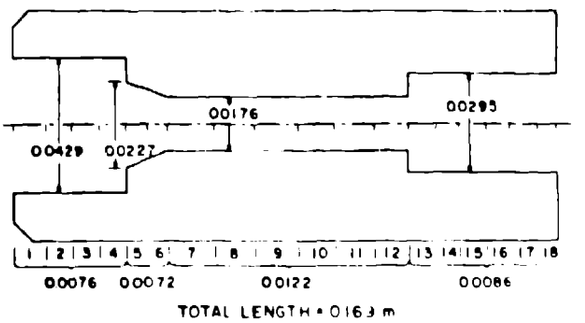

Fig. 5. Semiscale LOFT counterpart nozzle noding.

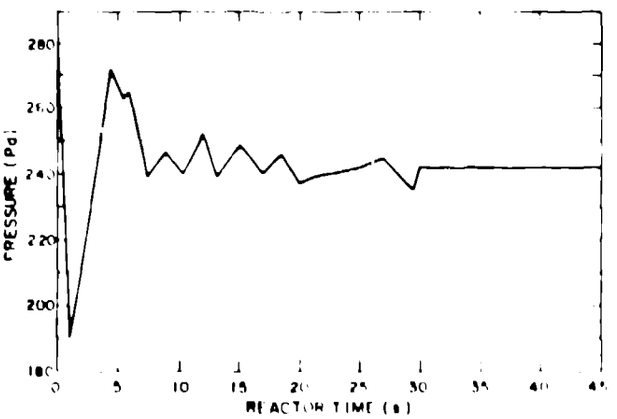

Fig. 6. Suppression tank back pressure.

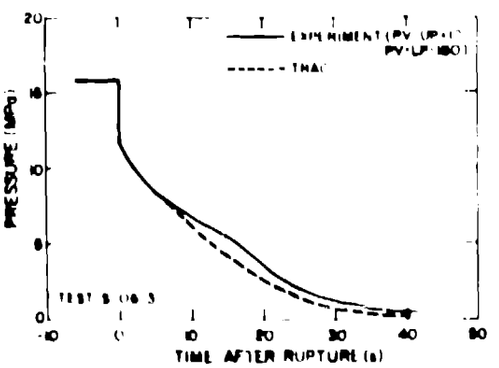

Fig. 7. Upper plenum pressure comparison.

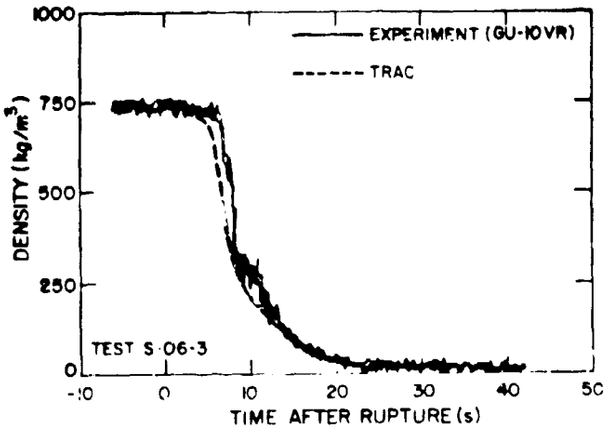

Fig. 8. Intact loop pump inlet density.

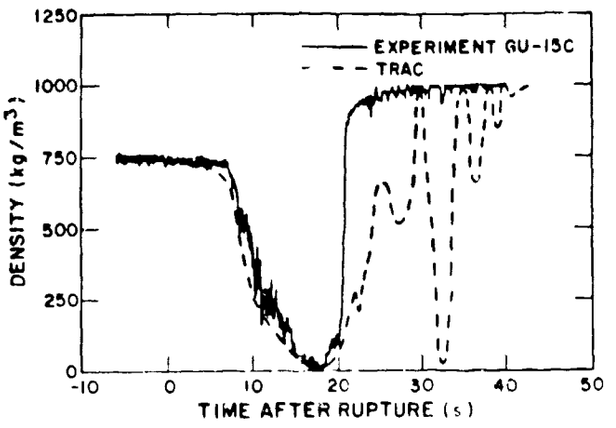

Fig. 9. Intact loop cold-leg density.

TABLE I

COMPARISON OF CALCULATED AND MEASURED INITIAL CONDITIONS

	Parameter	Calculated	Measured
1.	Initial power (75% of full power)	(input)	1.005 8 x 10⁷ W
2.	Pump speed (~ constant)	(input)	170.0 rad/s
3.	Power decay	(input)	time-dependent
4.	High-power-rod linear power	(input)	39.4 kW/m
5.	Low-power-rod linear power	(input)	24.9 kW/m
6.	Intact cold-leg flow rate	4.76	4.75 (kg/s)
7.	Core volumetric flow rate	0.007 34	0.007 04 (m^3/s)
8.	Upper plenum pressure	1.58 x 10^7	1.577 x 10^7 Pa
9.	Inlet fluid temperature to vessel	562.1	564.2 K
10.	Outlet fluid temperature from vessel	601.4	599.8 K
11.	Steam-generator secondary-side average fluid temperature	555.1	557.9 K
12.	Steam-generator secondary-side average pressure	6.6 x 10^6	6.57 x 10^6 Pa
13.	Steam-generator secondary-side flow rate	0.57	0.41 (kg/s)
14.	High-power-rod cladding temperature at midcore	694.4	690.0 K
15.	Low-power-rod cladding temperature at midcore	669.1	672.0 K
16.	ECC water temperature	(input)	510 K 0 ≤ t ≤ 20 s 301 K t > 20 s

TABLE II

TABLE OF EVENTS

	Event	Time (s)
1.	200% double-ended cold-leg break, reactor power tripped	0.0
2.	Begin HPIS flow	0.5
3.	Begin isolating steam generator secondary side	8.0
4.	Pressurizer empties (level below 0.1 m)	15.0
5.	Accumulator flow initiated	18.5
6.	High-power-rod first peak clad temperature reached (1 120 K)	20.0
7.	Steam-generator secondary-side inlet valve closed	22.0
8.	Begin LPIS flow, steam-generator secondary-side outlet valve closed	25.0
9.	High-power-rod second peak clad temperature reached (1 12[illegible] K)	51.0
10.	Bottom node of high-power rod quenched	64.0
11	Accumulator flow ends	90.0
12.	Low-power rod quenches (through core midplane)	130.0
13.	High-power rod quenches (through core midplane)	240.0

calculated intact loop cold-leg density begins to show some oscillations after 20 s. These oscillations are condensation induced and occur earlier in the calculation than in the experiment (these oscillations are observed later in the experiment). The oscillations occur in the code because the ECC system is modeled in TRAC with a short pipe connected to a flow boundary condition, whereas in the actual system, a complicated piping network connects the accumulator, LPIS, and HPIS to the intact cold leg, which in effect creates a time delay before the ECC water reaches the cold leg. In the TRAC calculation, however, this time delay is not accounted for, thus the ECC reaches the cold leg instantaneously. Figure 10 shows a comparison of the calculated and measured flow in the intact cold leg. Note that even though the intact cold-leg density calculation shows some oscillations (Fig. 9), the calculated flow is in excellent agreement with the experimental data (Fig. 10).

Comparisons of the pressurizer pressure and broken hot-leg pressure are shown in Figs. 11 and 12. Calculated values for those variables are generally in good agreement with the reported data. The underprediction of the pressure can be explained by Fig. 13, which shows the pressure drop across the simulated pump in the broken hot leg. Most of the pressure drop in the system occurs in this component. It is seen that the calculated pressure drop is somewhat lower than the data for the first 30 s of the transient. This can be attributed to the uncertainty in the loss coefficient reported (2) for the pump simulator orifice. The value used for the TRAC calculation was too low and resulted in a pressure drop that was too low during the single-phase liquid and early two-phase flow periods. This result coupled with the coarse noding in the core may explain why the TRAC calculation blows down at a faster rate than the experiment.

The calculated and experimental break flows are shown in Figs. 14 and 15. It is seen that the calculated hot-leg break flow is in reasonable agreement with the experimental data, whereas the calculated cold-leg break flow underpredicts the subcooled portion of the blowdown. This is caused by boiling in the nozzle, which decreases the flow.

Comparisons for the low-power and high-power rod cladding temperatures are shown in Figs. 16 and 17. These comparisons are for the middle core level (core midplane) at about the 0.74-m (29-in.) elevation. Double peaks in the clad temperature are observed in both the calculation and the measurements. The calculated magnitudes and times of each peak are in reasonable agreement with the data. The low-power rods quench about 20 s too early in the TRAC calculation whereas the high-power rods quench about 70 s too late. This phenomena can be attributed to the coarse noding used in the vessel. Because only one radial region together with two equal azimuthal sectors and three axial levels were used in the core, only two cells are available to receive flow from the lower plenum. The high-power rod was modeled in cell 1 of Fig. 2 and the low-power rod was modeled in cell 2. The intact cold leg supplies ECC water to cell 4 of Fig. 2 (adjacent to cell 2, low-power rod). As a result of this noding, slightly more flow is directed up through cell 2, compared to cell 1, from the lower plenum region, thus the low-power rod quenches too early in the calculation; and the high-power rod quenches too late. The high-power rods also quench too late because of the large change in the power step between core level 1 and core level 2 (see Figs. 2 and 3). If more axial nodes were to be used in the core, resulting in a smoother transition between power steps, the quench front would propagate faster and thus quench the rod earlier. If more azimuthal sectors were used in the vessel, a more uniform flow distribution would result at the core inlet, allowing a more uniform quench front propagation for both the low- and high-power rods.

CONCLUSIONS

The calculation described above took approximately 170 min of CPU time on the CDC 7600 for a 250-s transient. This is a substantial reduction (a factor of five) in running time for detailed problems of this type.

The results of the calculation are generally in good agreement with the measured data with the coarse vessel noding accounting for most of the major differences between the experimental data and the TRAC calculation. Based on these results it appears that coarse noding is adequate for relatively fast scoping calculations. A more detailed noding would improve the results at the expense of increased running times.

REFERENCES

1 "TRAC P1, An Advanced Best-Estimate Computer Program for PWR LOCA Analysis," Los Alamos Scientific Laboratory report LA-7279-MS (June 1978).

2 "Draft Experimental Data Report for Test S-06-3," EG&G Idaho, Inc. report.

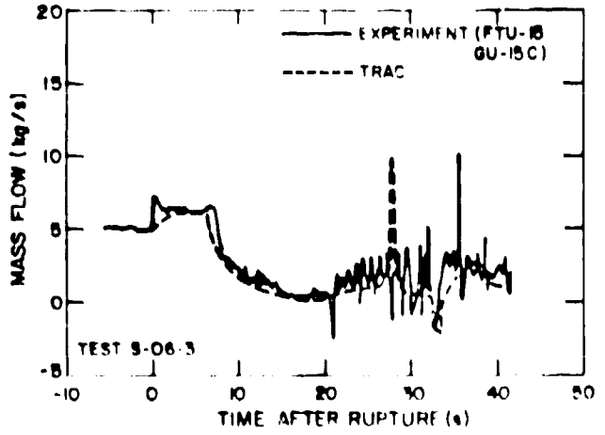

Fig. 10. Intact cold-leg flow rate.

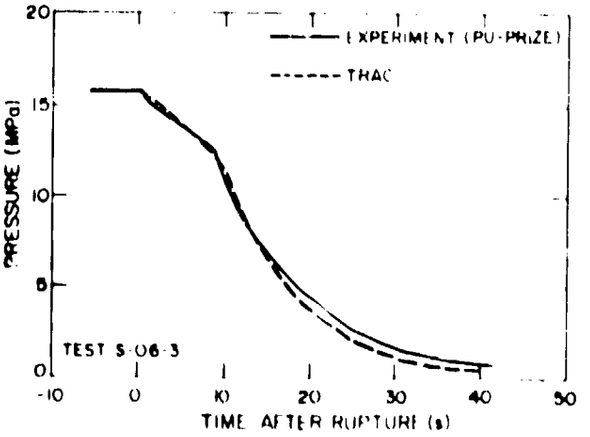

Fig. 11. Pressurizer pressure.

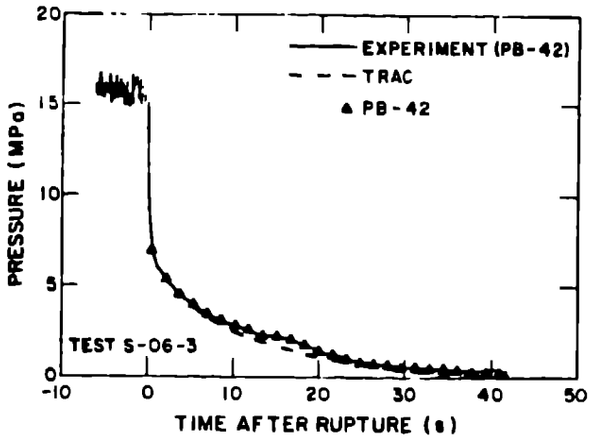

Fig. 12. Broken hot-leg pressure.

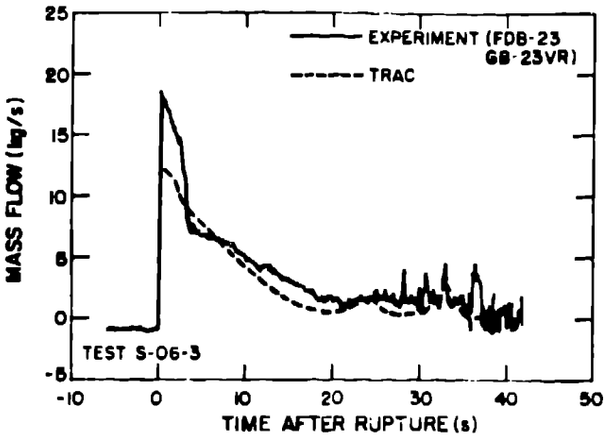

Fig. 15. Cold-leg break flow rate.

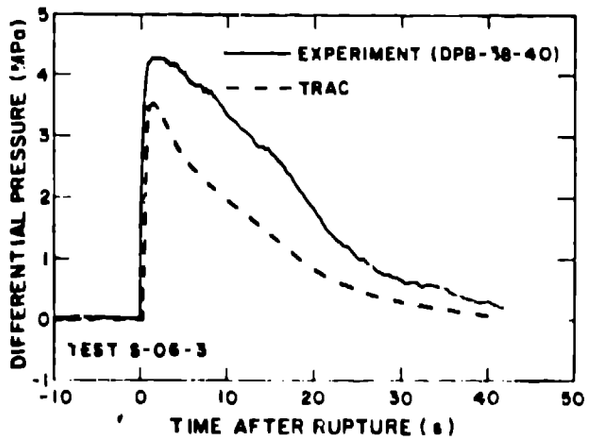

Fig. 13. Pressure drop across pump simulator in broken hot leg.

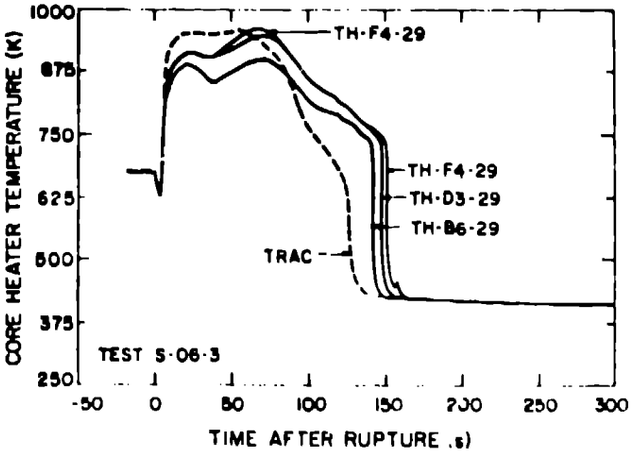

Fig. 16. Low-power rod cladding temperature.

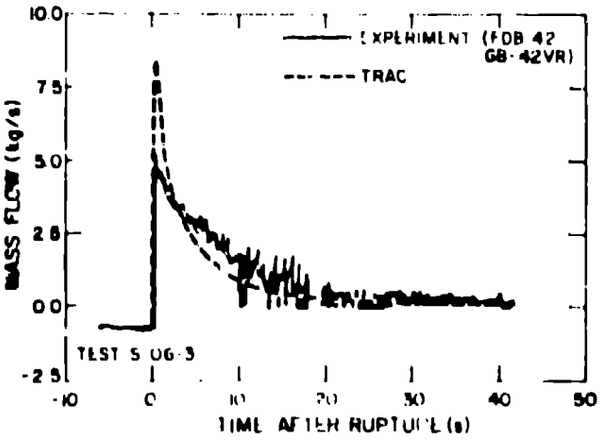

Fig. 14. Hot leg break flow rate.

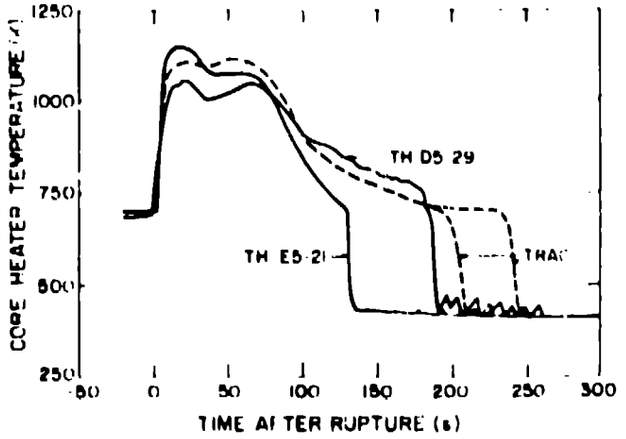

Fig. 17. High power rod cladding temperature.